

Novel heat-flux scaling for convection at low winds

R Narasimha and Kusuma G Rao*

Fluid Dynamics Unit, Jawaharlal Nehru Centre for Advanced Scientific Research
also National Institute of Advanced Studies

Bangalore India

email: roddam@nias.iisc.ernet.in

*Space Sciences, Indian Space Research Organization, Bangalore, India

MEGHA-TROPIQUES 2nd Scientific Workshop, 2-6 July 2001, Paris, France.

Abstract

An analysis of atmospheric observational data indicates that the conventionally defined drag and heat transfer coefficients increase rapidly as wind speed falls. It is shown here that, at low winds, (i) there is a *linear* increase of drag with wind speed and (ii) the observed heat flux is independent of wind speed. These findings are not consistent with the so-called free-convection limit of Monin-Obukhov theory. They are instead best seen as the result of a new regime of ‘weakly forced convection’, in which the heat flux is determined solely by temperature differentials as in free convection, and the momentum flux by a perturbation linear in wind on free convection. This regime is governed by a new velocity scale determined by the heat flux (rather than by the friction velocity as in classical turbulent boundary layer theory). Novel definitions of the drag and heat exchange coefficients, based on appropriate heat-flux velocity scales, are found to be independent of wind speed at low winds. The height of the capping inversion in this regime is proportional to the surface heat flux, and is determined by a simple argument balancing energy supply at surface to rate of work done to lift air parcels to inversion height.

1 Introduction

The most widely used approach for taking into account the effect of stratification on a turbulent boundary layer is based on Monin-Obukhov (M-O) similarity theory. This theory has been extensively discussed in both the fluid-dynamical and meteorological literature [1,2].

The theory has in general received extensive support from field observations, and is widely used in atmospheric and oceanographic modelling. However, there has been much discussion about the inadequacy of M-O theory in the limit of free convection. In general the observed bulk aerodynamic coefficients increase as wind speed falls (as noted by Bradley, Coppin and Godfrey [3] from measurements over the West Pacific, and by Kusuma Rao, Narasimha and Prabhu [4] from measurements over land); and, as the latter reference points out, the observed fluxes at low winds are much higher than predicted by M-O theory.

Indeed, the problem of low-wind fluxes is currently of great meteorological interest following the finding of Miller, Beljaars and Palmer [5] that simulations of tropical climate (including in particular the Indian monsoons) are substantially better with an enhancement of low-wind fluxes over the values given by parameterization schemes earlier in use at the European Centre for Medium-range Weather Forecasts. One common practice of atmospheric modellers to take account of low-wind conditions has been to introduce a ‘gustiness’ parameter, which replaces

the low surface winds generated in the models by some specified higher value (usually in the range $1\text{--}3\text{ ms}^{-1}$: see Hack *et al.* [6]), and continues to use M-O theory at the specified cut-off velocity.

The chief purpose of the present study is to show that the fluid dynamics of low-wind eddy fluxes in the atmosphere is best seen as characterizing a regime of weakly forced convection. This view produces meaningful scaling laws for heat and momentum fluxes and the inversion height at low winds in the atmosphere.

2 Background

The problem of estimating surface heat flux in turbulent convection under conditions of vanishingly small mean flow has a long history. Thus, Townsend [7] writes the surface heat flux in free convection in the form

$$Q_s = C_s \rho_0 C_p \left(\frac{g}{\theta} \frac{\kappa^2}{\nu} \right)^{1/3} (\Delta\theta)^{4/3}, \quad (1)$$

where κ is the molecular thermal diffusivity, ν the kinematic viscosity and $\Delta\theta$ the difference in potential temperature between the surface and the mixed layer. C_s is a constant whose value was estimated to be 0.2 by Townsend [7], and as lying in the range 0.1 to 0.24 by Deardorff and Willis [8]. Equation (1) is equivalent to the heat flux relation $\text{Nu} \sim \text{Ra}^{1/3}$ in terms of the Nusselt (Nu) and Rayleigh (Ra) numbers, generally considered appropriate for smooth surfaces.

Recently Kusuma Rao *et al.* [4,9] have shown that atmospheric observations over land during the experiment known as MONTBLEX-90 [10–12] reveal a rapid rise in drag as well as heat exchange coefficient at low winds (although at different rates). While at higher winds there is good agreement between M-O theory and observations, at low winds there is substantial disagreement (amounting to as much as 30% in the friction velocity U_* , for example; see Figure 4, [4]), showing that the theory is inadequate in the nearly windless free convection limit.

In particular, Kusuma Rao *et al.* [9] have shown that the sensible heat flux measurements made during MONTBLEX-90 obey free convection scaling, being consistent with a $4/3$ power law on an appropriate temperature differential, as in (1). Interestingly, it was further shown that the (dimensional) drag depends almost linearly on wind speed, but the implications of these findings on similarity theory were not discussed. Since their study, Kondo and Ishida [13] have also reported a similar $4/3$ power law for the sensible heat flux, for experiments conducted either indoors or in the field.

3 Observational data analysed

The data analysed here come from three atmospheric experiments. For the MONTBLEX data, Rudrakumar, Ameenullah and Prabhu [14] present a detailed description of the tower instrumentation, the associated data acquisition system and the various quality checks adopted to ensure the reliability of acquired data. The sensors providing the data were mounted on a 30 m high guyed uniform triangular lattice structure, with booms fitted at 6 levels (1, 2, 4, 8, 15, 30 m above the surface). The data used in the present analysis were acquired at Jodhpur ($26^\circ 18' \text{ N}$, $73^\circ 04' \text{ E}$) over a period extending from 9 June to 20 August. A sonic anemometer was placed at a height of 4m above the surface, cup anemometers at all the six heights mentioned above, and platinum wire resistance thermometers at the four heights 1, 8, 15 and 30 m. The total number of data sets acquired during the period was 676.

The tower was installed in a farm field, which at the time of the observations reported here was covered with small pebbles or patches of grass. A detailed description of the tower site is given by Kusuma Rao [15]. The momentum roughness length was estimated at an average value of 1.23 cm in the sector between 200° to 230° , which was relatively flat with no obstacles on the ground; this sector will be called the ‘smooth’ sector in the following. In the rest of the site covered by the prevailing wind directions the roughness length was somewhat higher, at an average value of 4.5 cm; this will be called the ‘rough’ sector.

Important supplementary data come from the boundary layer field experiment BLX83 carried out between 26 May and 18 June 1983 near Chickasha, Oklahoma ($35^\circ 02' \text{ N}$, $97^\circ 51' \text{ N}$) using the NCAR aircraft Queenair [16], and from measurements carried out on board ORV *Sagar Kanya* during the Indian Ocean Experiment INDOEX carried out in 1998 [17], and reported by Manghnani *et al.* [18].

4 Assessment of M-O theory at low winds

Figure 1 shows that the momentum flux estimated from M-O theory for MONTBLEX data tends to vary (as may be expected) in proportion to the square of the wind speed, almost all the way up to $U_{10} \sim 8 \text{ ms}^{-1}$.

A similar plot for the M-O estimate of the heat flux Q_s (Figure 2) shows almost no correlation with the wind speed. These estimates will be compared below with observations.

5 The sensible heat flux

Figure 3 shows the heat flux variation with the characteristic temperature differential $\Delta\theta$ taken as the difference between values at 1 m and 30 m above surface, the lowest and highest levels at which data are

available from the MONTBLEX tower. (Note that at the relatively small values of z we are considering, the virtual temperature θ is practically identical with the ordinary temperature T .) The data collapse very well in the plot of $Q_s^{3/4}$ against $\Delta\theta$, as suggested by (1); the best fit is $Q_s^{3/4} = 29.0(T_1 - T_{30}) [\pm 11.6]$ (here and in the sequel this notation stands for the best fit $[\pm$ the root mean square deviation from the best fit]).

There is some indication that the heat flux is slightly different between the rough and smooth sectors, the best fits being

$$Q_s^{3/4} = 28.0(T_1 - T_{30}) [\pm 15.01]$$

and

$$Q_s^{3/4} = 30.0(T_1 - T_{30}) [\pm 8.4]$$

respectively. Note the significantly lower scatter in the smooth sector: the heat flux itself is affected little. The result is not sensitive to the choice of other temperature differentials derived from the tower data.

What is remarkable about Figure 3 is that the scatter seen in Figure 2 is dramatically reduced; even at wind speeds of order 8 m s^{-1} , the heat flux seems to depend only on the temperature differential, and not on the wind speed.

6 The momentum flux

The momentum flux, computed by the eddy correlation technique as $-\rho \overline{U'w'}$, where U' is the fluctuation in the horizontal wind speed along the mean wind direction, is shown as a function

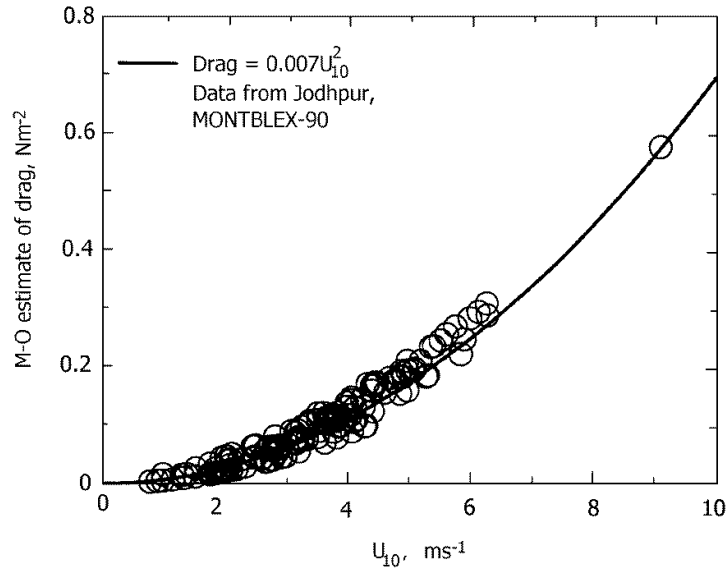


Figure 1: Estimates of drag provided by Monin-Obukhov theory for values of mean velocity and temperature gradient derived from measurements in MONTBLEX-90. Curve shows a least-squares fit to the estimate.

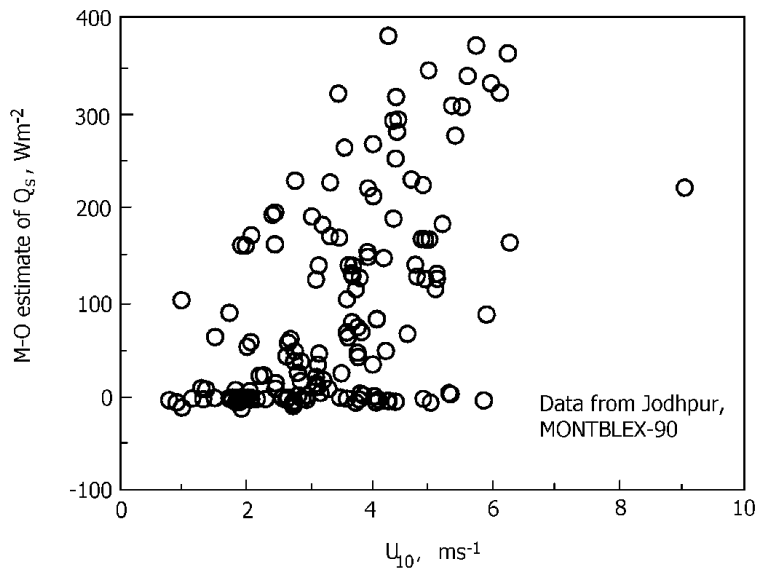


Figure 2: Estimates of sensible heat flux provided by Monin-Obukhov theory as in Figure 1, showing that no trend can be discerned with mean wind.

of wind speed U_{10} in Figure 4, for points from the smooth sector. It is seen that the drag varies linearly with wind speed ($0.047U_{10} [\pm 0.089]$) to a very good approximation, even at wind

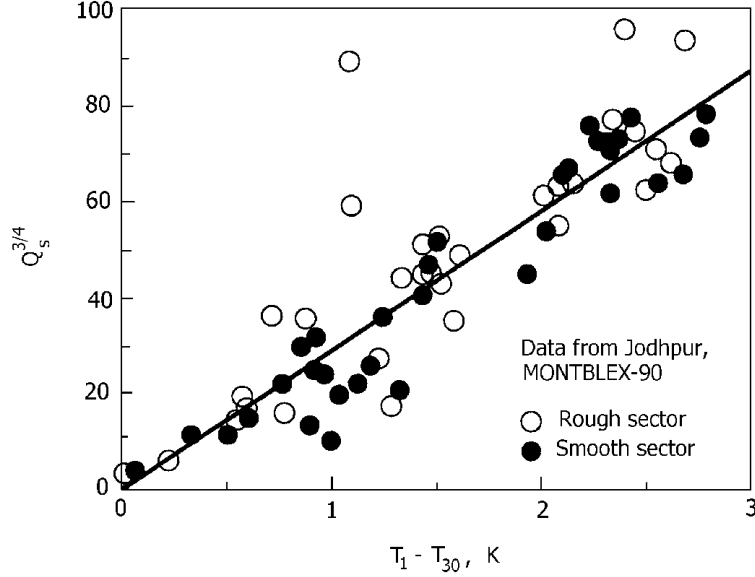


Figure 3: Observed sensible heat flux (MONTBLEX data) as a function of a characteristic temperature differential, showing a 4/3 power dependence

speeds of up to 8 m s^{-1} . (The corresponding relation is $0.051U_{10} [\pm 0.10]$ in the rough sector and $0.050U_{10} [\pm 0.097]$ overall : the drag is slightly higher in the rough sector.) By comparison with Figure 1 it is clear that virtually all the measured flux values lie above the M-O prediction curve. Indeed, the momentum flux, and consequently the drag, does not follow M-O theory but is instead proportional to the first power of U_{10} – i.e. (as already pointed out by Kusuma Rao *et al.* [4]), the drag coefficient $C_D (\equiv -\overline{U'w'}/U_{10}^2) \sim U_{10}^{-1}$ to a first approximation.

Taken together with the result for heat flux shown in Figure 3, these results show that wind is acting as a linear perturbation on the free convection regime, producing virtually no effect on the heat flux but generating a first-order momentum flux as a departure from a pure free-convection regime where the net drag vanishes at zero wind.

7 New velocity scales

The above results strongly suggest that eddy fluxes at low winds are best seen as constituting a new thermal flow regime that we shall call nearly free or weakly forced convection. We propose that in this regime, which in the limit has $U_* \rightarrow 0$, $\overline{U'w'} \rightarrow 0$ but $\overline{w'T'} \rightarrow 0$, the scaling is driven primarily by the non-vanishing surface heat flux Q_s .

Using the heat flux as the primary variable (and not the drag, as in M-O theory), two new velocity scales may be defined, respectively as

$$U^{\wedge} = \frac{Q_s}{\rho_0 c_p \Delta\theta} \quad (2)$$

and

$$U^{\sim} = \frac{\overline{T}^{1/3}}{\rho_0 c_p} \frac{Q_s}{(\Delta\theta)^{4/3}} = U^{\wedge} (\Delta\theta/\overline{T})^{-1/3}. \quad (3)$$

The velocity scale U^{\wedge} may be seen as a measure of the *vertical* velocity that generates the heat flux Q_s . The second velocity scale U^{\sim} differs from the first by the factor $(T/\Delta\theta)^{1/3}$, and is

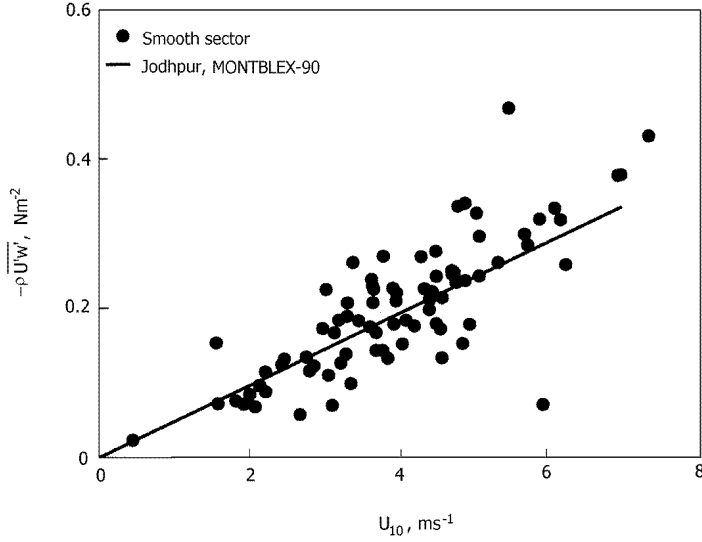


Figure 4: Observed drag as a function of wind speed

inspired by the 4/3 power law for the heat flux expressed by equation (1). The two velocity scales are displayed in Figure 5 as a function of wind speed U_{10} . It is seen that U^{\sim} has a value $0.476 [\pm 0.0017] \text{ ms}^{-1}$, virtually independent of wind speed. This is to be expected, and merely confirms that the 4/3 power law (1) is accurately obeyed. The velocity scale $U^{\hat{}}$, on the other hand, varies between 0.02 and 0.11 ms^{-1} , and shows no simple direct correlation with wind speed; from the invariance of U^{\sim} we deduce that $U^{\hat{}} \sim (\Delta\theta/\bar{T})^{1/3}$. We shall find below that both scales may have their uses.

It is immediately seen that a modified heat exchange coefficient defined as

$$C_H^{\hat{}} = \frac{Q_s}{\rho_0 C_p U^{\hat{}} \Delta\theta} \quad (4)$$

will, by definition, be unity independent of wind speed. On the other hand, a coefficient defined as

$$C_H^{\sim} = \frac{Q_s}{\rho_0 C_p U^{\sim} \Delta\theta} \quad (5)$$

shows a slow variation with wind speed, given by the relation $C_H^{\sim} = 0.147(U_{10}/U^{\sim})^{0.14}$. (These graphs are not shown as they would convey no information that is not already displayed in Figure 3.)

We now introduce two new candidates for a definition of the drag coefficient,

$$C_D^{\hat{}} = \frac{D}{\rho_0 U^{\hat{}} U_{10}}, \quad C_D^{\sim} = \frac{D}{\rho_0 U^{\sim} U_{10}} \quad (6)$$

where $D = -\rho_0 \overline{U'w'}$ represents drag. These definitions incorporate the observed linear dependence on U_{10} , and utilize the heat-flux velocity scales for non-dimensionalization. Figure 6 shows the variation, with wind speed, of the newly defined drag coefficients. Here the wind speed is normalized by the appropriate heat flux velocity scale ($U_{10}/U^{\hat{}}$ or U_{10}/U^{\sim}). In presenting data points for these drag coefficients we have rejected those for which $\Delta\theta < 0.05^\circ\text{C}$; such a threshold is based on the limited accuracy of the temperature data, and is within the

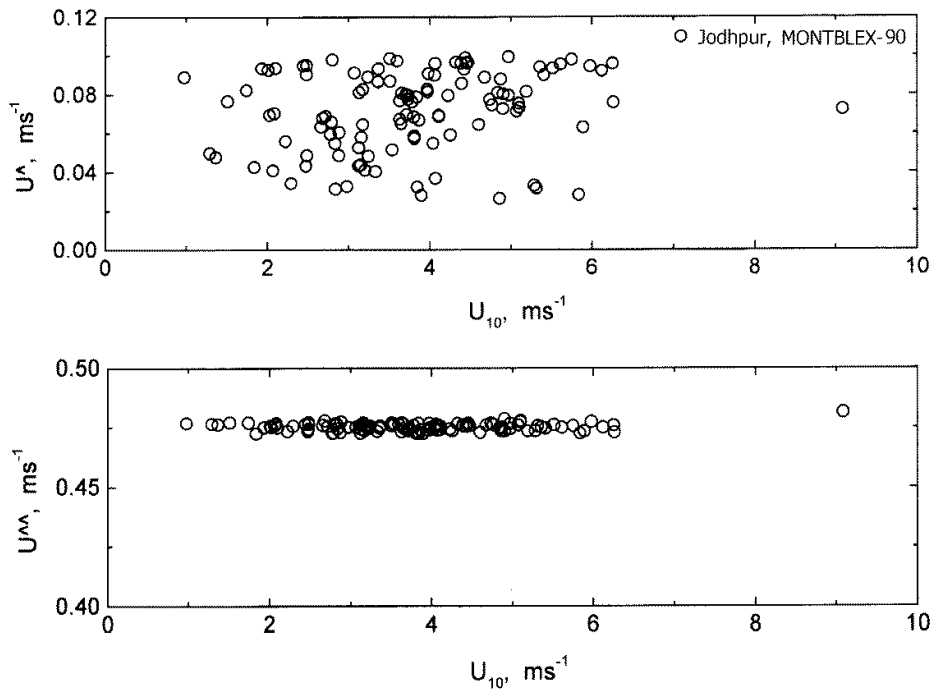


Figure 5: Variation with wind speed of the two candidates for a heat-flux velocity scale

noise level of the measurements. (Note that if the reported $\Delta\theta$ is negative, so will \hat{U} be in the definition adopted here.) From Figure 6, we see that \hat{C}_D shows a slow rise with wind speed ($\simeq 0.006U_{10} + 0.28 [\pm 0.27]$), whereas C_D is nearly constant, at about 0.089. This lack of wind dependence suggests that the new velocity scale (2) is the most appropriate for drag parameterization. The scaling is effective for both smooth and rough sectors.

The drag coefficient \hat{C}_D is found to remain independent of wind speed irrespective of the temperature differential used in the definition of \hat{U} ; its actual value however depends on the choice of ΔT .

It is seen that the range of wind speed over which the weakly forced convection regime prevails, as determined from the drag, extends at least up to $U_{10}/\hat{U} \approx 18$.

8 Height of capping inversion

The height Z_i of the capping inversion plays a direct role in some current models for the fluxes at low winds. The present approach however has already demonstrated that the fluxes can be seen as scaling with

local parameters, provided the heat flux rather than momentum flux is taken as the primary characterising variable. This leaves the height of the capping inversion to be determined – presumably as a parameter that responds directly to the surface heat flux Q_s .

We propose here that Q_s directly determines the potential energy corresponding to the inversion height, namely gZ_i . Unfortunately MONTBLEX data do not provide Z_i . However, two recent sets of data on Z_i are available from BLX-83 and INDOEX [16,18]. The two sets cover heat fluxes ranging from less than 5 Wm^{-2} to more than 200 Wm^{-2} , and are plotted together in Figure 7. This diagram suggests that there is a close connection between Z_i and Q_s . As the wind

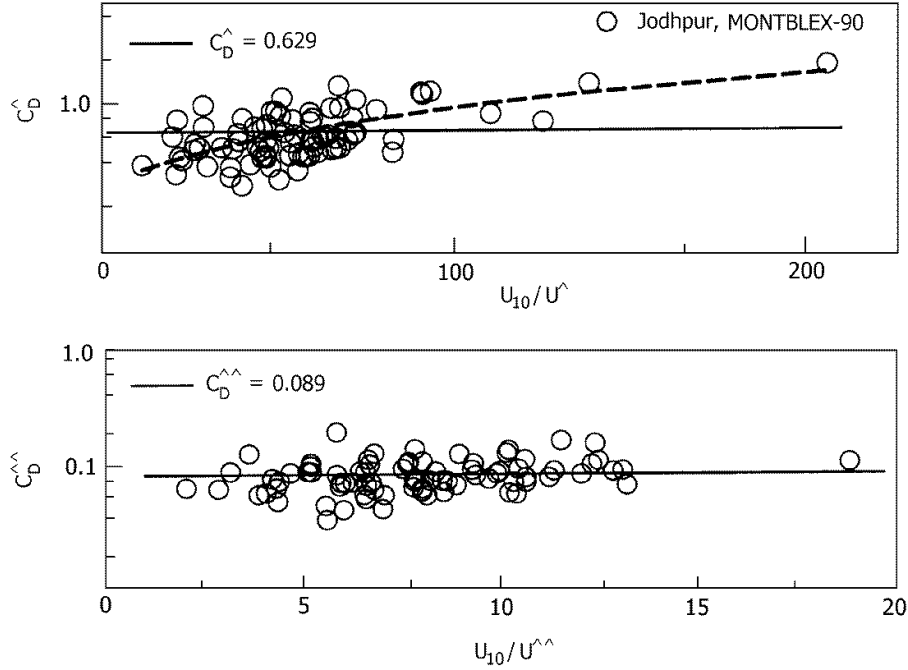


Figure 6: Drag data using two new definitions of drag coefficient, involving respectively the two heat-flux velocity scales \hat{U} , $\hat{\hat{U}}$ defined in text. Upper panel shows increasing trend, lower panel shows that a constant value of \hat{C}_D is a good approximation.

velocities involved are in the range 1 to 10 ms^{-1} , they provide test cases for the present arguments, according to which the heat-flux velocity scales should play a strong role in determining Z_i . This suggests that one should seek relations between the non-dimensional heights

$$\frac{gZ_i}{\hat{U}^2} \quad \text{or} \quad \frac{gZ_i}{\hat{\hat{U}}^2}$$

and the non-dimensional heat flux

$$\frac{Q_s}{\rho_0 \hat{U}^3} \quad \text{or} \quad \frac{Q_s}{\rho_0 \hat{\hat{U}}^3}.$$

A plot of the latter is shown in Figure 8 (the former also plots almost as well). A linear relationship can be seen, which can be expressed as

$$\frac{gZ_i}{\hat{\hat{U}}^2} = 3.56 \frac{Q_s}{\rho_0 \hat{\hat{U}}^3} + 0.023 [\pm 0.077] \quad (7)$$

As temperature differentials are not available from Manghnani *et al.* [18], their data cannot be plotted on Figure 8, but Figure 7 already indicates that the INDOEX data and the BLX3 data may be expected to be consistent with each other from this point of view.

Indeed, (7) suggests a simple direct energetic relationship between Z_i and Q_s , for at sufficiently large Q_s the small intercepts in (7) can be omitted, and we can write

$$Z_i \simeq 3.56 \frac{Q_s}{\rho_0 g \hat{\hat{U}}^2} \quad (8)$$

which implies that the inversion height Z_i is determined by the rate at which the energy supply Q_s at the surface can work to lift air parcels against gravity to that height.

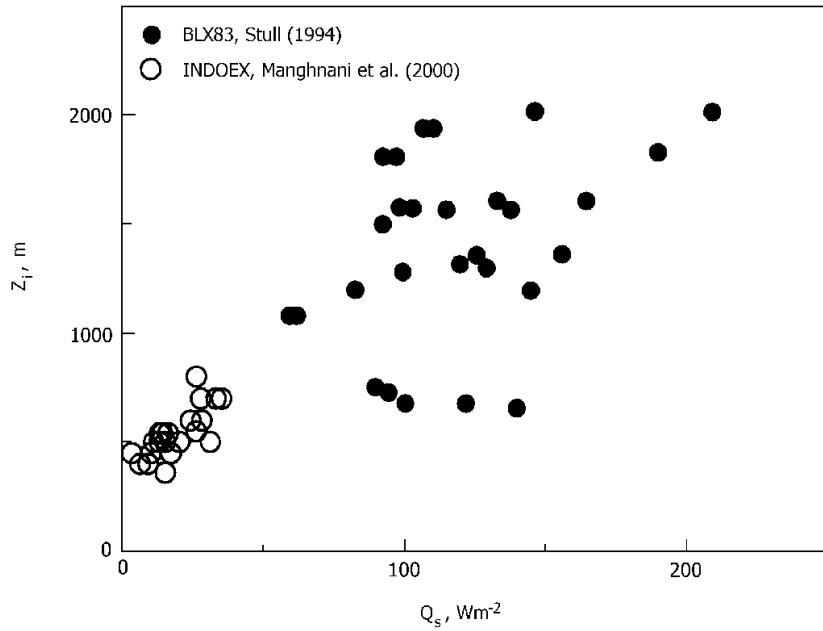


Figure 7: Capping inversion height as function of heat-flux, data of Manghnani *et al.* [18]

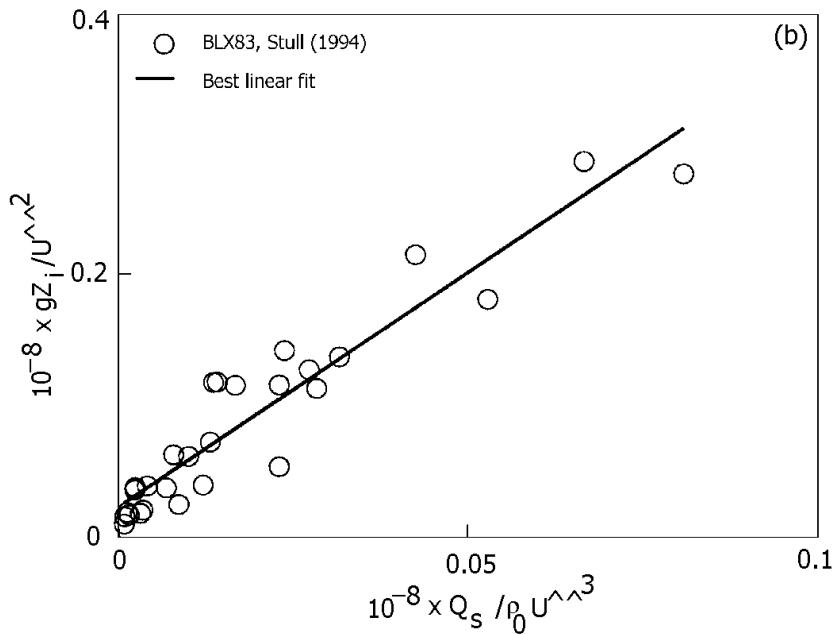


Figure 8: Dependence of capping inversion height Z_i on the heat flux, in the present heat-flux scaling. (Observational data from Stull [16].)

9 Conclusion

We have shown here, by an analysis of atmospheric data, that at low winds classical Monin-Obukhov theory, and in particular its limit as $U_* \rightarrow 0$, is unable to account for certain major characteristics of the eddy fluxes of momentum and heat. The observations show that, even at

wind speeds of upto 8 m s^{-1} at a height of 10 m, the heat flux shows no strong correlation with wind speed, whereas the momentum flux varies *linearly* with wind speed. Monin-Obukhov theory cannot predict these marked features of the observed fluxes at low winds.

On the other hand, the theory proposed here postulates a regime of weakly forced or nearly free convection, in which the heat flux depends only on temperature differentials (and not on wind), and the momentum flux results from a linear perturbation on windless free convection. This suggests new heat-flux-based velocity scales for the flow; the classical friction velocity U_* , in the limit when it is small, is not relevant from this point of view. A drag coefficient based on the new heat-flux velocity scale is virtually independent of wind speed upto $\sim 8 \text{ m s}^{-1}$, showing a new kind of similarity in the weakly-forced convection regime. Furthermore, the height of the capping inversion is shown to be determined by a simple energy relationship, equating heat input at surface to the rate at which energy has to be expended to lift air parcels to the inversion height. The view implicit in the scaling proposed here is thus that the fluxes can generally be scaled on the basis of parameters close to the surface; the resulting velocities determine the overall boundary layer parameters.

10 References

1. Haugen, D.A. (ed.) (1973) *Workshop on Micrometeorology*. American Meteorological Society, Boston, Massachusetts, USA
2. Stull, R.B. (1988) *An Introduction to Boundary Layer Meteorology*. Kluwer Academic Publications, Amsterdam.
3. Bradley, E.F., Coppin, P.A. and Godfrey, J.S. (1991) Measurements of sensible and latent heat flux in the western equatorial Pacific Ocean. *J. Geophys. Res. (Suppl.)* **96**, 3375–3389.
4. Kusuma G. Rao, Narasimha, R. and Prabhu, A. (1996a) Estimation of drag coefficient at low wind speeds over the monsoon trough land region during MONTBLEX-90. *Geophysical Research Lett.* **23**, 2617–2620.
5. Miller, M.J., Beljaars, A.C.M. and Palmer, T.N. (1992) The sensitivity of the ECMWF model to the parameterization of evaporation from the tropical oceans. *J. Climate* **5**, 418–434.
6. Hack, J.J., Boville, B.A., Briegleb, B.P, Kiehl, J.T., Rasch, P.J. and Williamson, D.L. (1993) Description of the NCAR Community Climate Model (CCM2). *NCAR Tech. Note*, NCAR/TN-382+STR, NTIS PB93-221802/AS. Climate and Global Dynamics Division, National Center for Atmospheric Research, Boulder, Colorado.
7. Townsend, A.A. (1964) Natural convection on water over an ice surface. *Q.J.R. Meteorol. Soc.* **90**, 248–259.
8. Deardorff, J.W. and Willis, G.W. (1985) Further results from a laboratory model of the convective planetary boundary layer. *Boundary-Layer Meteorol.* **32**, 205–236.
9. Kusuma G. Rao, Narasimha, R. and Prabhu, A. (1996b) An analysis of MONTBLEX data on heat and momentum flux at Jodhpur. *Proc. Indian Acad. Sci. (E&PS)* **105**, 309–323.

10. Goel, M. and Srivastava, H.N. (1990) Monsoon Trough Boundary Layer Experiment (MONTBLEX). *Bull. Am. Meteorol. Soc.* **71**, 1594–1600.
11. Sikka, D.R. and Narasimha, R. (1995) Genesis of the monsoon trough boundary layer experiment (MONTBLEX). *Proc. Indian Acad. Sci. (Earth Planet. Sci.)* **104**, 157–187.
12. Narasimha, R., Sikka, D.R. and Prabhu, A. (1997) *The Monsoon Trough Boundary Layer*. Indian Academy of Sciences, Bangalore.
13. Kondo, J. and Ishida, S. (1997) Sensible heat-flux from the Earth's surface under natural convective conditions. *J. Atmos. Sci.* **54**, 498–509.
14. Rudrakumar, S., Ameenulla, S. and Prabhu, A. (1995) MONTBLEX tower observations: Instrumentation, data acquisition and data quality. *Proc. Indian Acad. Sci. (Earth Planet. Sci.)* **104**, 221–248.
15. Kusuma G. Rao (1996) Roughness length and drag coefficient at two MONTBLEX-90 tower stations. *Proc. Indian Acad. Sci. (Earth Planet. Sci.)* **105**, 273–287.
16. Stull, R.B. (1994) A convective transport theory for surface fluxes. *J. Atmos. Sci.* **51**, 3–22.
17. Mitra, A.P. (1999) INDOEX (India): Introductory note. *Current Sci.* **76**, 886–889.
18. Manghnani, V, Sethuraman, Niyogi, D.S., Parameshwara, V., Morrison, J.M., Ramana, S.V. and Raju, J.V.S. (2000) Marine boundary layer variability over the Indian ocean during INDOEX (1998). *Boundary Layer Meteorology*, **97**, 411–430.